Cu^{2+} and AMP complexation of enlarged tripodal polyamines†

M. Teresa Albelda,[a] Enrique García-España,*[a] Hermas R. Jiménez,[b] José M. Llinares,[c] Conxa Soriano,*[c] Alejandra Sornosa-Ten[a] and Begoña Verdejo[a]

Received 20th April 2006, Accepted 22nd June 2006
First published as an Advance Article on the web 10th July 2006
DOI: 10.1039/b605639c

The synthesis, characterization, Cu^{2+} coordination and interaction with AMP of three tripodal polyamines are reported. The polyamines are based on the structure of the tetraamine (tren) which has been enlarged with three propylamino functionalities (**TAL**), with a further anthrylmethyl fragment at one of its terminal primary nitrogens (**ATAL**) or with naphthylmethyl fragments at its three ends (**N3TAL**). The protonation constants of all three polyamines show that at pH 6, all six primary and secondary nitrogen atoms in the arms are protonated. The interaction with Cu^{2+} and AMP (adenosine-5′-monophosphate) has been studied by potentiometric, UV-Vis, ESI-MS spectroscopy and NMR techniques. pH-Metric, NMR and ESI/MS techniques indicate that **TAL** and **ATAL** form with AMP adducts of 1 : 1, 2 : 1 and 3 : 1 AMP : L stoichiometries in water. This is one of the first examples for the formation of such complexes in aqueous solution. Formation of ternary complexes between **TAL**, **ATAL**, **N3TAL**, Cu^{2+} and AMP is observed. Paramagnetic NMR techniques have been used to obtain structural information on the binding mode of AMP to the Cu^{2+}–**TAL** binuclear complexes.

Introduction

Polyamines are water-soluble ambivalent receptors capable of interacting with metal ions and anionic species. Coordinative interactions with metal ions will occur when the pH is high enough to allow for a sufficiently large number of available electron pairs. Interaction with anionic or polar species will be mainly driven by electrostatic interactions when the pH is low enough for having a sufficiently high number of protonated amino groups within the receptor. Additionally, if the polyamine has a high number of nitrogens appropriately distributed, intermediate situations in which the polyamine is able to interact with metal ions and anions in separated compartments can also be envisaged. All these binding modes can be modulated by the length of the hydrocarbon chains between the amino groups as well as by the attachment of aromatic functionalities. The large structural variability of polyamines and the pH regulation of their binding modes allow for many applications such as selective metal or anion complexation and detection.[1–3] A particularly interesting point is the development of ligands interfering selectively with structures and functions of nucleic acids.[4] The conformational changes of such ligands induced by Cu^{2+} ions can lead to dramatic allosteric effects in their association with double stranded DNA.[5]

Variation of the number and location of the protonated nitrogen atoms allows for controlling the amount and density of positive charges, which has a profound influence on the interactions with nucleic acids. Introduction of condensed aromatic moieties into such polyamines leads to stacking effects with nucleobases and in particular to intercalation into double stranded nucleic acids.

A particularly high concentration of ammonium centers is accessible with tripodal derivatives containing a large number of nitrogen atoms. In this respect the tripodal polyamine tris(2-aminoethyl)amine (tren) constitutes one of the most useful and widely employed building block.[6]

Here, we report on the synthesis, characterization, Cu^{2+} coordination and interaction with adenosine-5′-monophosphate (AMP) of three receptors of this class. In these receptors the polyamine tren has been enlarged with three aminopropyl functionalities (**TAL**), and further functionalised with an anthrylmethyl fragment at one of its terminal primary nitrogens (**ATAL**) or with naphthylmethyl fragments at its three ends (**N3TAL**) (See Chart 1).[7]

[a]*Departament de Química Inorgànica, Institut de Ciència Molecular (ICMOL), Universitat de València. Edificio de Institutos de Paterna, Apartado de Correos 22085, 46071, Valencia, Spain. E-mail: enrique.garcia-es@uv.es; Tel: 963544879*
[b]*Departament de Química Inorgànica, Facultat de Química, Universitat de València, 46100, Burjassot, Valencia, Spain*
[c]*Departament de Química Orgànica, Institut de Ciència Molecular (ICMOL), Facultat de Farmàcia, Universitat de València, 46100, Burjassot, Valencia, Spain*

† Electronic supplementary information (ESI) available: Fig. S1: Distribution diagrams for the systems: (A) H^+–**TAL**; (B) H^+–**ATAL**; (C) H^+–**N3TAL**. Table S1: Observed chemical shifts for the interaction of AMP with the tripodal ligands **TAL** and **ATAL**. Table S2: Logarithms of the equilibrium constants for the interaction of AMP with the tripodal polyamines **TAL**, **ATAL** and **N3TAL**. Table S3: ^{1}H NMR hyperfine-shifted resonances and temperature dependence of Cu_2**TAL**, Cu_2**TAL**–AMP complexes in D_2O at 25 °C and pH 8. Fig. S2: Distribution diagrams for the system AMP–**TAL**: [**TAL**] = 1×10^{-3} mol dm^{-3}, [AMP] = 1×10^{-3} mol dm^{-3}. Fig. S3: Distribution diagrams for the system AMP–**TAL**: [**TAL**] = 1×10^{-3} mol dm^{-3}, [AMP] = 3×10^{-3} mol dm^{-3}. Fig. S4: Distribution diagrams for the system AMP–**ATAL**: [**ATAL**] = 1×10^{-3} mol dm^{-3}, [AMP] = 2×10^{-3} mol dm^{-3}. Fig. S5: Distribution diagrams for the system AMP–**ATAL**: [**ATAL**] = 1×10^{-3} mol dm^{-3}, [AMP] = 3×10^{-3} mol dm^{-3}. Fig. S6: Distribution diagrams for the ternary system Cu^{2+}–**TAL**–AMP: (A) [Cu^{2+}] = [**TAL**] = [AMP] = 1×10^{-3} mol dm^{-3}; (B) [Cu^{2+}] = 2×10^{-3} mol dm^{-3}, [**TAL**] = [AMP] = 1×10^{-3} mol dm^{-3}. Fig. S7: Distribution diagrams for the ternary system Cu^{2+}–**ATAL**–AMP: (A) [Cu^{2+}] = [**ATAL**] = [AMP] = 1×10^{-3} mol dm^{-3}; (B) [Cu^{2+}] = 2×10^{-3} mol dm^{-3}, [**ATAL**] = [AMP] = 1×10^{-3} mol dm^{-3}. Fig. S8: Distribution diagrams for the ternary system Cu^{2+}–**N3TAL**–AMP: [Cu^{2+}] = [**N3TAL**] = [AMP] = 1×10^{-3} mol dm^{-3}. See DOI: 10.1039/b605639c

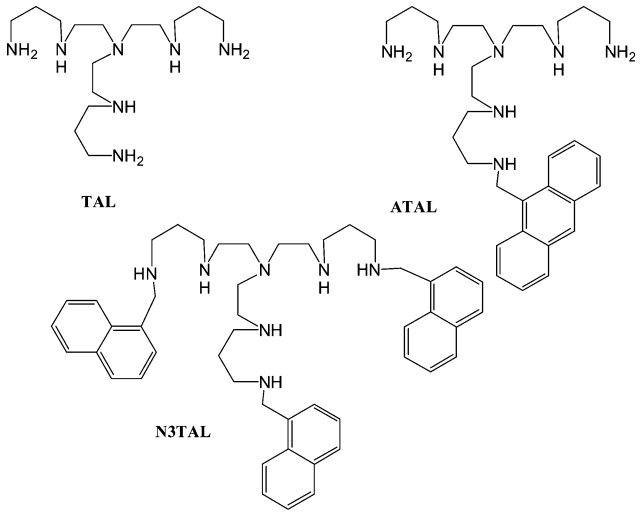

Chart 1

Synthesis of polyamine compounds

TAL, **ATAL** and **N3TAL** were prepared following the general synthetic strategy delineated in Scheme 1, which consists of tosylation of tris(2-aminoethyl)amine (**1**) and reaction of tris(tosylated) derivative (**2**) with *N*-(3-bromopropyl)-phthalimide to give the enlarged compound (**3**). Compound (**3**) is then treated with hydrazine to remove the protection (compound (**4**)) and with an HBr–AcOH–PhOH mixture to give the detosylated amine as its hydrobromide salt (**TAL**·6HBr). The solid obtained was washed extensively with ethanol to yield **TAL**·6HBr in a pure form as confirmed by elemental microanalysis and spectroscopic data.

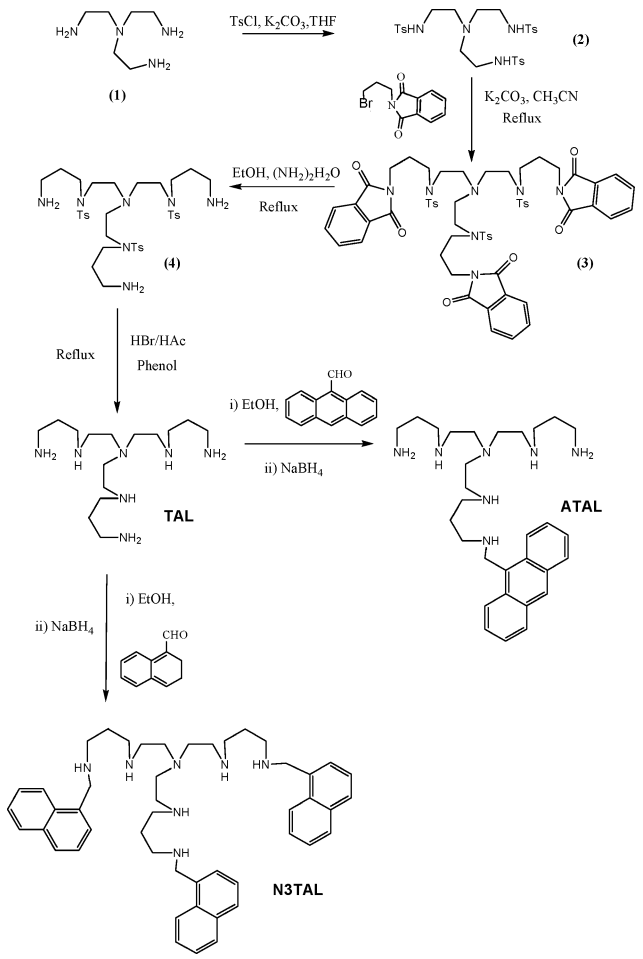

Scheme 1 Synthesis pathway for the preparation of **TAL**, **ATAL** and **N3TAL**.

In order to obtain the terminally functionalized tripodal ligands, we reacted **TAL** in its free amine form with the corresponding anthracene or naphthalene carbaldehydes. For preparing **ATAL**, in which the fluorophore was appended to just one of the arms of **TAL**, a molar ratio anthracene-9-carbaldehyde : **TAL** of 1 : 3 was used whereas for obtaining the tripodal compound **N3TAL**[8] with all its three arms functionalized with methylnaphthyl groups, a reverse molar ratio naphthalene-1-carbaldehyde : **TAL** of 3 : 1 was used. The overall yield is large enough to obtain the compounds in a gram scale.

Protonation behaviour

Table 1 collects the stepwise protonation constants for the three tripodal ligands determined at 298.1 K in 0.15 mol dm^{-3} NaCl and Fig. S1 (ESI†) the distribution diagram for the species existing in equilibrium.

All three ligands present six relatively high basicity constants followed by a much lower one for the seventh protonation step (Table 1 and Fig. S1, ESI†). On the other hand, the basicity displayed by the non-substituted polyamine is clearly higher than those of the substituted derivatives given the basicity order **TAL** > **ATAL** > **N3TAL**. All these facts can be interpreted taking into account repulsive interactions between same sign charges, the inductive effects generated by the different substituents, the different hydration of the compounds and possible hydrogen bond formation.

It is well established that electrostatic repulsion between positive charges separated by propylenic chains is considerably lower than when the separation is by ethylenic chains.[9] This is the reason for the relatively small decrease in basicity observed in every one of the six first protonations of all three ligands. The very low seventh protonation constant would correspond to protonation of the apical nitrogen atom. It is interesting to remark that although these last constants are small, they can be determined or estimated potentiometrically, in contrast with the polyamine tren for which just three protonation constants could be measured

Table 1 Logarithms of the stepwise protonation constants for the ligands **TAL**, **ATAL** and **N3TAL** determined at 298.0 ± 0.1 K in 0.15 mol dm^{-3} NaCl

Reaction[a]	TAL	ATAL	N3TAL[c]
$L + H \leftrightarrow HL$	10.34(7)[b]	10.41(3)	9.08(6)
$HL + H \leftrightarrow H_2L$	10.26(2)	9.87(2)	8.70(5)
$H_2L + H \leftrightarrow H_3L$	9.52(4)	9.17(3)	8.48(5)
$H_3L + H \leftrightarrow H_4L$	8.68(4)	8.02(3)	7.76(4)
$H_4L + H \leftrightarrow H_5L$	7.91(5)	7.2(3)	7.09(5)
$H_5L + H \leftrightarrow H_6L$	7.37(4)	5.78(8)	6.80(4)
$H_6L + H \leftrightarrow H_7L$	2.2(1)	<2.00	2.25(9)

[a] Charges omitted. [b] Numbers in parenthesis are standard deviations in the last significant figure. [c] Taken from ref. 8.

by potentiometry.[10] The general decrease of basicity observed for the compounds with the aromatic rings **ATAL** and **N3TAL** can be ascribed to a poorer stabilization by hydration of the ammonium groups in the more hydrophobic environments.

Interaction with Cu^{2+} ions

The equilibrium constants for the formation of Cu^{2+} complexes with **TAL**, **ATAL** and **N3TAL** are included in Table 2. **TAL** displays the highest stability constants followed by the mono(anthrylmethyl) derivative **ATAL** while **N3TAL** is the polyamine presenting the lowest stability constants with Cu^{2+}. $[Cu(\mathbf{TAL})]^{2+}$ has three protonation constants from which the first two are high and comparable to the protonation constants of the free ligand while the third one is much lower. On the other hand the stability constant for the $[CuL]^{2+}$ complex of **TAL** is clearly higher than that reported for the parent polyamine tris(2-aminoethyl)amine (tren) ($\log K_{ML} = 19.58$) in which its four nitrogens are involved in the coordination to the metal ion.[11,12] These data suggest a coordination number of five for the Cu^{2+}–**TAL** complexes. The visible spectra of the system Cu^{2+}–**TAL** were recorded at pH values where the different mononuclear and binuclear species predominate in solution (see distribution diagrams in ESI†). For 1 : 1 molar ratio the spectra of the two main species in solution, $[Cu(H_2\mathbf{TAL})]^{4+}$ and $[Cu(\mathbf{TAL})]^{2+}$, are practically identical consisting of a wide band centred at 740 nm (ε = 270 M^{-1} cm^{-1}) preceded by a shoulder at 600–620 nm. These spectral features are characteristic of a trigonal bipyramidal geometry.[11] The absence of changes between the spectra of these two species confirms that the protonation processes occur on nitrogen atoms not involved in the coordination to the metal.

The analysis of the species formed in the system Cu^{2+}–**ATAL** reflects similar tendencies whereas the results are somewhat different for the system Cu^{2+}–**N3TAL**. First, a tetraprotonated $[Cu(H_4\mathbf{N3TAL})]^{6+}$ complex has also been detected. In second place, the constant for the third protonation step, $[Cu(H_2L)]^{4+} + H^+ = [Cu(H_3L)]^{5+}$, is much higher for **N3TAL** than for the other two polyamines. These along with the lower constant found for the $[Cu(\mathbf{N3TAL})]^{2+}$ complex suggest four coordinated nitrogens in this system. Analogously to the system Cu^{2+}–**TAL** the UV-Vis spectra indicate a rhombic geometry for the system Cu^{2+}–**N3TAL** with a very broad band centered at around 740 nm and a shoulder at *ca.* 620 nm.

Table 2 Logarithms of the stability constants for the formation of Cu^{2+} complexes with the ligands **TAL**, **ATAL** and **N3TAL** determined at 298.0 ± 0.1 K in 0.15 mol dm^{-3} NaCl

Reaction[a]	TAL	ATAL	N3TAL
Cu + L ↔ CuL	22.91(4)[b]	19.08(4)	16.21(7)
CuL + H ↔ CuHL	9.52(3)	10.34(2)	8.37(4)
CuHL + H ↔ CuH_2L	9.21(2)	8.60(1)	7.55(2)
CuH_2L + H ↔ CuH_3L	3.96(2)	4.81(2)	6.60(3)
CuH_3L + H ↔ CuH_4L			3.92(5)
2 Cu + L ↔ Cu_2L	30.75(6)[c]		
Cu_2L + H_2O ↔ $Cu_2L(OH)$ + H	−9.82(3)		
$Cu_2L(OH)$ + H_2O ↔ $Cu_2L(OH)_2$ + H	−10.17(6)		

[a] Charges omitted. [b] Numbers in parentheses are standard deviations in the last significant figure. [c] Values determined in 0.15 mol dm^{-3} $NaClO_4$.

Therefore, in all the mononuclear Cu^{2+} complexes there are non-coordinated nitrogen atoms that might permit the coordination with a further metal ion. However, in NaCl medium addition of a further mole of Cu^{2+} ion leads, in all three cases, to precipitation, and formation of binuclear complexes is not detected. When changing the ionic strength to $NaClO_4$ containing the less coordinating ClO_4^- counter-anions,[13] formation of the binuclear Cu^{2+} complexes $[Cu_2(\mathbf{TAL})]^{4+}$, $[Cu_2(\mathbf{TAL})(OH)]^{3+}$ and $[Cu_2(\mathbf{TAL})(OH)_2]^{2+}$ is observed for **TAL** while for the other two systems precipitation still persists. For a Cu^{2+}–**TAL** mol ratio 2 : 1, the binuclear species predominate in aqueous solution at pH values over 7.0. The UV-vis spectra recorded for a 2 : 1 Cu^{2+} : **TAL** mol ratio, although more intense, show similar characteristics to those of the mononuclear species with the presence of a band at 740 nm and an hypsochromically shifted shoulder at around 607 nm.

Interaction with AMP

In order to explore the possibility to use the metal complexes for simultaneous detection of nucleotides and to better understand how the interaction with the nucleic acids occurs[7] an analysis of the interaction of the receptors with adenosine-5′-monophosphate (AMP) was carried out.

Table 3 collects the corresponding data for the tripodal receptors. An interesting feature is that the tripodal polyamines **TAL** and **ATAL** are able to form AMP : L adduct complexes of 2 : 1 and 3 : 1 stoichiometries. Such stoichiometries have been checked following the variations of the ^{31}P NMR chemical shifts of AMP when increasing amounts of **TAL** were added. The measurements have been conducted in a pH region close to the first pK_a of AMP.[14] The effects of the AMP–L interaction will be an increase in the apparent basicity of the polyamine and in the apparent acidity of the anionic guest and thus the changes will be more noticeable in

Table 3 Logarithms of the equilibrium constants for the interaction of AMP ($AMP^{2-} \equiv A$) with the tripodal polyamines **TAL**, **ATAL** and **N3TAL** determined at 298.0 ± 0.1 K in 0.15 mol dm^{-3} NaCl

Reaction[a]	TAL	ATAL	N3TAL
A + HL ↔ HLA	5.17(5)[b]	6.37(6)	6.28(1)
A + H_2L ↔ H_2LA	5.02(5)	6.56(7)	6.02(9)
A + H_3L ↔ H_3LA	5.22(5)	6.63(6)	6.30(1)
A + H_4L ↔ H_4LA	5.28(5)	6.80(6)	6.15(8)
A + H_5L ↔ H_5LA	5.38(5)	7.15(6)	6.42(9)
A + H_6L ↔ H_6LA	5.36(4)	7.65(7)	6.23(8)
HA + H_5L ↔ H_6LA	6.41(4)	7.11(4)	6.71(8)
HA + H_6L ↔ H_7LA	3.78(5)		4.92(8)
2 A + H_5L ↔ H_5LA_2	8.09(1)		
2 A + H_6L ↔ H_6LA_2	8.25(9)		
2 HA + H_5L ↔ H_7LA_2	9.45(8)		
A + HA + H_5L ↔ H_7LA_2	8.40(8)		
2 HA + H_6L ↔ H_8LA_2	7.42(5)	8.01(1)	
A + H_5LA ↔ H_5LA_2	2.74(5)		
A + H_6LA ↔ H_6LA_2	2.89(4)		
3 A + H_5L ↔ H_5LA_3	11.83(6)		
3 A + H_6L ↔ H_6LA_3	12.10(5)	14.52(8)	
A + H_5LA_2 ↔ H_5LA_3	3.74(6)		
A + H_6LA_2 ↔ H_6LA_3	3.85(5)		
2 A + HA + H_6L ↔ H_7LA_3	12.31(5)		
A + 2 HA + H_6L ↔ H_8LA_2	12.07(5)		
3 HA + H_6L ↔ H_9LA_3	10.87(4)		

[a] Charges omitted. [b] Numbers in parentheses are standard deviations in the last significant figure.

such a region. The ^{31}P NMR chemical shift of the system AMP–**TAL** at pD = 6.5 shows significant changes for AMP : **TAL** molar ratios 3 : 1, 2 : 1 and 1 : 1 with downfield shifts of 1.7, 2.1 and 3.1 ppm, respectively, with respect to the non-complexed AMP (see Table S1, ESI†). For AMP : **TAL** molar ratios lower than 1 : 1, no further changes in chemical shift were observed. Similar results are obtained for the system AMP : **ATAL** (Table S1, ESI†). However, although in the case of **ATAL** formation of 2 : 1 and 3 : 1 AMP : L adduct species was also detected (see Table 3), the pH range of formation of such species was narrower (see distribution diagrams in Fig. S4 and S5, ESI†). Finally, in the case of the polyamine with the three arms functionalised with naphthylmethyl groups, the 2 : 1 and 3 : 1 AMP–L species were not detected either by potentiometric or NMR methods.

ESI-MS spectra recorded in the positive mode for the system AMP–**TAL** (Fig. 1) shows peaks at *m*/*z* 665.4, 1012.5 and 1359.5 attributable to the ionic species $[H_3(\mathbf{TAL})(AMP)]^+$, $[H_5(\mathbf{TAL})(AMP)_2]^+$ and $[H_7(\mathbf{TAL})(AMP)_3]^+$, respectively supporting the formation of adduct species of 1 : 1, 2 : 1 and 3 : 1 AMP : L stoichiometries.

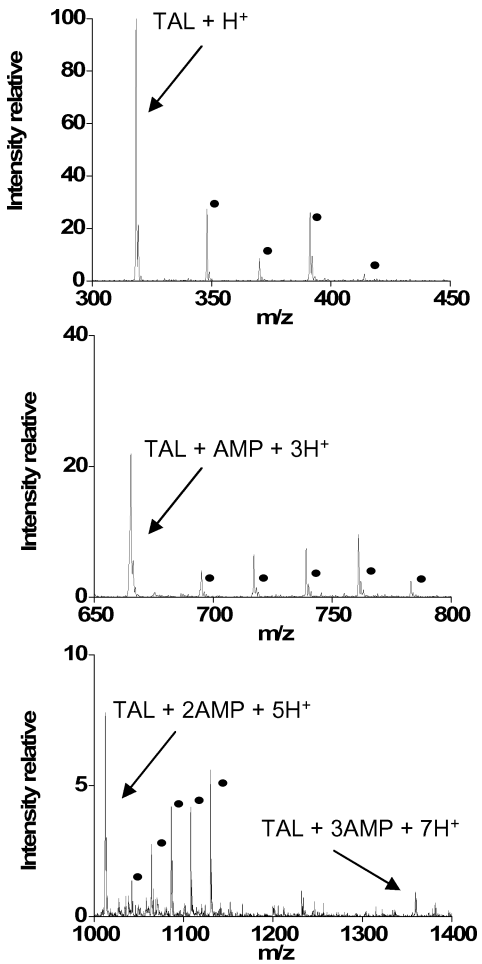

Fig. 1 ESI (positive mode) mass spectra without fragmentation for the system AMP–L (●, AMP). The peaks corresponding to the adduct complexes are marked with arrows.

In order to compare the AMP·L adduct formation constants for the different systems care must be taken in comparing the correct equilibrium and values of stability constants (Table 3). Since both AMP and the receptors participate in overlapping proton transfer processes, translating the cumulative stability constants into representative stepwise constants requires to consider the basicities of AMP[14] and of the different ligands and assume that the interaction will not affect much the pH range of existence of the protonated species of AMP and L. If this is taken into account, the stepwise constants shown in Table 3 can be deduced as representative of the equilibria occurring in solution (the complete set of cumulative constants is collected in Table S2, ESI†).

It deserves to be mentioned that the interactions presented by all three polyamines are among the highest found for synthetic receptors.[15] It is interesting to note that in contrast to what happens in the systems Cu^{2+}–tripodal polyamines, **N3TAL** and **ATAL** interact more strongly with AMP than **TAL**. π–π-Stacking interactions could contribute to enhance the affinity of **ATAL** and **N3TAL** for AMP with respect to **TAL**. Additionally, the hydrophobic environment generated by the aryl moieties would lower the local dielectric constant and thus reinforce electrostatic interactions between the oppositely charged partners.

Perhaps, the most striking feature of the chemistry of these ligands is the above mentioned formation of 2 : 1 and particularly, 3 : 1 AMP : L species by **TAL** and **ATAL**.

Interestingly, when one compares the stepwise constants for the equilibria $AMP^{2-} + H_6L^{6+} = [H_6L(AMP)]^{4+}$, $\log K_1 = 5.36$; $AMP^{2-} + [H_6L(AMP)]^{4+} = [H_6L(AMP)_2]^{2+}$, $\log K_2 = 2.89$ and $AMP^{2-} + [H_6L(AMP)_2]^{2+} = [H_6L(AMP)_3]$, $\log K_3 = 3.85$, the trend $K_1 > K_2 < K_3$ is found (Table 3). The same occurs when analysing the constants for the successive addition of AMP to the pentaprotonated receptor $AMP^{2-} + H_5L^{5+} = [H_5L(AMP)]^{3+}$, $\log K_1 = 5.38$; $AMP^{2-} + [H_5L(AMP)]^{3+} = [H_5L(AMP)_2]^{+}$, $\log K_2 = 2.74$ and $AMP^{2-} + [H_5L(AMP)_2]^{+} = [H_5L(AMP)_3]^{-}$, $\log K_3 = 3.74$ (Table 3). This trend can be explained taking into account that all three arms are coinvolved in the binding of the first AMP molecule (Scheme 2(A)). The entrance of the second AMP would imply an opening of the receptor due to electrostatic repulsions between the two anions (Scheme 2(B)). The third AMP will find an adequate arrangement for binding and the constant will again increase (see Scheme 2(C)).

Ternary complexes Cu^{2+}–L–AMP

In order to shed light on how the preformed Cu^{2+} complexes might interact with the phosphate groups of the nucleic acids,[5,7] we have analysed by potentiometry, UV-Vis and paramagnetic NMR the formation of Cu^{2+}–L–AMP mixed complexes. The relevant data is presented in Table 4 and Fig. 2 shows the distribution diagram for the system Cu^{2+}–**N3TAL**–AMP in 2 : 1 : 1 molar ratio. The other distribution diagrams are collected in Fig. S6, S7 and S8 of the ESI.† **TAL**, **ATAL** and **N3TAL** form mono- and dinuclear Cu^{2+}–L–AMP species in aqueous solution.

Formation of dinuclear complexes are favoured by the presence of the nucleotide which provides additional binding sites for the anchoring of the second metal ion. For instance, while no binuclear complexes are observed in the binary system Cu^{2+}–**N3TAL**, in the presence of the nucleotide it has been possible to detect a very stable $[Cu_2(\mathbf{N3TAL})(AMP)]^{2-}$ complex (see Fig. 2).

^1H paramagnetic NMR measurements have been performed in order to gain further insight about the interaction of

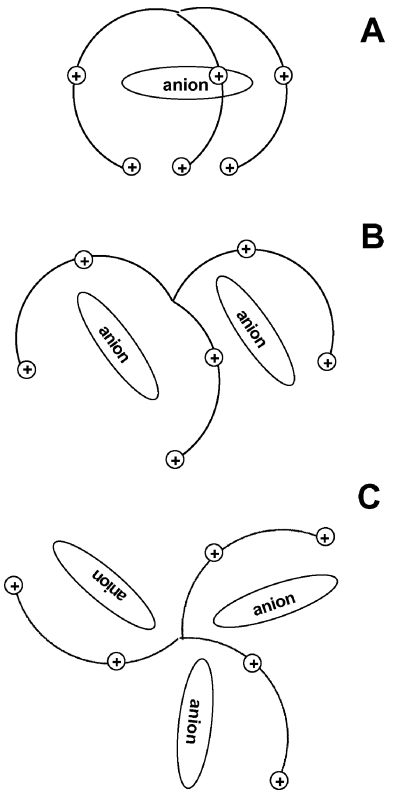

Scheme 2 Schematic representation of the interaction between hexaprotonated **TAL** and AMP.

Table 4 Logarithms of the equilibrium constants for the interaction of Cu^{2+} and AMP ($AMP^{2-} \equiv A$) with the polyamines **TAL**, **ATAL** and **N3TAL** determined at 298.0 ± 0.1 K in 0.15 mol dm^{-3} NaCl

Reaction	TAL	ATAL	N3TAL
Cu + A + L ↔ CuAL[a]		23.58(7)	21.7(1)
Cu + A + H +L ↔ CuHAL	36.00(9)[b]	33.71(7)	30.3(1)
Cu + A + 2 H + L ↔ CuH_2AL	45.37(6)	42.31(7)	37.9(1)
Cu + A + 3 H + L ↔ CuH_3AL	52.20(2)	43.39(2)	44.7(1)
Cu + A + 4 H + L ↔ CuH_4AL	55.99(3)		50.72(5)
Cu + A + 5 H + L ↔ CuH_5AL			55.10(7)
2 Cu + A + L ↔ Cu_2AL		31.89(7)	29.13(8)
2 Cu + A + H + L ↔ Cu_2HAL	43.06(3)	39.95(5)	
2 Cu + A + L + OH ↔ $Cu_2(OH)AL$		22.61(7)	
CuL + A ↔ CuAL		4.51(7)	5.60(6)
CuHL + A ↔ CuHAL	3.46(4)	4.30(3)	5.86(5)
CuH_2L + A ↔ CuH_2AL	3.49(3)	4.29(3)	5.90(4)
CuH_2L + HA ↔ CuH_3AL	4.30(1)	5.05(1)	6.28(4)
CuH_3L + HA ↔ CuH_4AL	4.68(2)		5.66(2)
CuH_2L + H_2A ↔ CuH_4AL	4.17(2)		8.35(2)
CuH_4L + HA ↔ CuH_5AL			6.12(3)
CuH_3L + H_2A ↔ CuH_5AL			6.13(3)
CuHAL + Cu ↔ Cu_2HAL	7.21(4)	6.24(4)	
CuAL + Cu ↔ Cu_2AL		8.31(4)	7.4(1)
CuA + CuHL ↔ Cu_2HAL	7.52(1)	7.38(2)	

[a] Charges omitted. [b] Numbers in parentheses are standard deviations in the last significant figure.

Cu^{2+}–**TAL** binuclear complexes with AMP. The ^1H NMR spectrum of the system Cu^{2+}–**TAL** in a 2 : 1 molar ratio recorded in D_2O at pH = 8 shows, in the downfield region, three well resolved isotropically shifted signals (a), (b), (c) and one non-resolved signal (B), Fig. 3(A). Additionally, it displays one upfield shifted signal

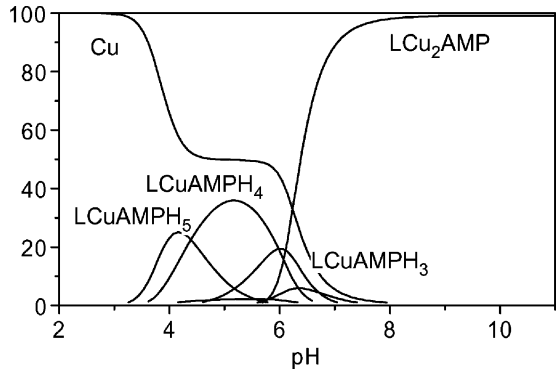

Fig. 2 Distribution diagram for the ternary system Cu^{2+}–**N3TAL**–AMP: $[Cu^{2+}] = 2 \times 10^{-3}$ mol dm^{-3}, [AMP] = [L] = 10^{-3} mol dm^{-3}.

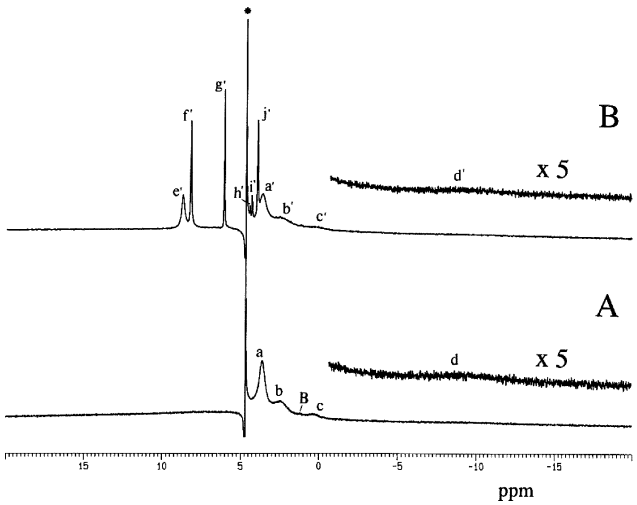

Fig. 3 400 MHz proton NMR spectra in D_2O at 298 K of (A) Cu_2–**TAL** at pH = 8, (B) Cu_2–**TAL**–AMP at pH = 8. The asterisks mark the residual solvent (*H_2O).

(d). The values of the chemical shift, linewidths at half-height and longitudinal relaxation times (T_1) are reported in Table 5. The peak linewidths measured at half-height are *ca.* ~200 Hz for all signals, except for signal (d) which has average linewidth of 1624 Hz. The signals (b), (c) and (d) which appear at 2.4, 0.28 and −9.3 ppm integrate twenty-four protons and exhibit very short T_1 values (<1 ms) can be assigned to the α-CH_2 protons (see Scheme 3).

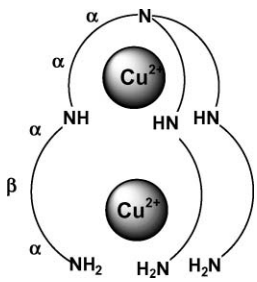

Scheme 3

The signal that appears at 3.6 ppm (a) integrates for six protons and exhibits a short T_1 value (3.7 ms) can be assigned to the remaining aliphatic protons of the tripodal polyamine (β-CH_2). The pattern of paramagnetic signals suggests a coordination for

Table 5 ^{1}H NMR hyperfine-shifted resonances of Cu_2**TAL**, Cu_2**TAL**–AMP complexes in D_2O at 25 °C and pH 8

Complex	Signal	δ/ppm	No. of protons	Assignment	T_1/ms	$\Delta\nu_{1/2}$/Hz	T_2[a]/ms
Cu_2**TAL**	a	3.6	6	β-CH_2 (**TAL**)	3.7	150	2.1
	b	2.4			<1	[b]	[b]
	B	1.2	24	α-CH_2 (**TAL**)	[b]	[b]	[b]
	c	0.28			<1	341	0.93
	d	−9.3			<1	1624	0.20
Cu_2**TAL**–AMP	a′	3.6	6	β-CH_2 (**TAL**)	2.5	195	1.6
	b′	2.5			<1	[b]	[b]
	c′	0.27	24	α-CH_2 (**TAL**)	<1	361	0.88
	d′	−9.2			<1	1131	0.28
	e′	8.7	2 × 2	γ-CH_2 (AMP)	11.2	78	4.1
	g′	6.1	2 × 2	$H_{2/8}$ CH (AMP)[c]	48.7	18	17.7
	f′	8.2			45.4	30	10.6
	h′	4.4	4 × 2	δ–σ-CH (AMP)[c]	36.8	[b]	[b]
	i′	4.3			35.3	[b]	[b]
	j′	3.9			21.9	24	13.3

[a] Measured from the line width at half-height. [b] Overlap prevents measurement of this value. [c] Tentative assignments.

two coppers ions such as that depicted in Scheme 3. As previously described,[16–18] spin-coupled binuclear Cu^{2+} complexes have similar short T_1 values and broad linewidths.

In the ^{1}H NMR spectrum of the ternary system Cu_2**TAL**–AMP in D_2O at pH = 8, not only new signals (e′–j′) appear, Fig. 3(B), but also the values of the proton longitudinal relaxation time are relatively larger, ranging from 11.2 ms for the signal (e′) to 48.7 ms for the signal (g′) (see Table 5).

The new group of signals can be assigned on the basis of integrated protons and of the longitudinal relaxation times of the hyperfine-shifted resonances. Signal (e′), which integrates four protons and exhibit the shortest T_1 value of the new signal group (11.2 ms) can be assigned to the γ-CH_2 AMP protons closest to the dicopper site (see Scheme 4). For the other group of signals (f′–j′), the specific assignment is given in Table 5.

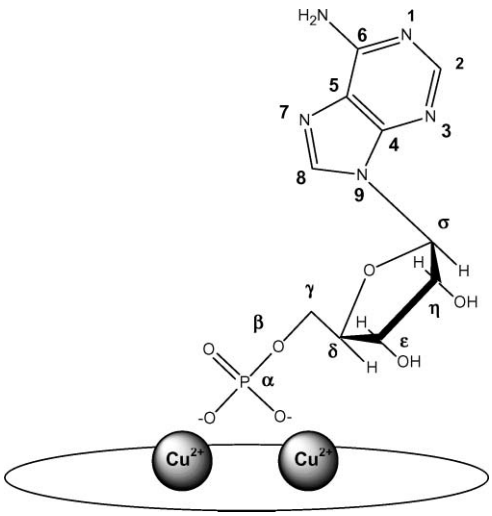

Scheme 4

These results are in accordance with a binding occurring through the phosphate group and support an Cu–O–O–Cu ligation mode for AMP (see Scheme 4). A Cu–N–N–Cu ligation mode through the adenine group would present a different pattern of chemical shifts with respect to the H_2 and H_8 AMP protons. The integration of the signals in measurements performed with different Cu_2**TAL** : AMP molar ratios have allowed for establishing the stoichiometries of the ternary complexes. The results show formation of ternary 1 : 1 and 1 : 2 complexes.

In order to obtain the temperature dependence of the hyperfine-shifted resonances, variable-temperature ^{1}H NMR spectra of the systems Cu_2**TAL** and Cu_2**TAL**:AMP in D_2O were registered from 283 to 323 K. All the signals of the two systems follow an anti-Curie behavior excepting the broad signals (d and d′) that show a Curie behavior (see Table S3 of the ESI†). It is important to note that the anti-Curie behavior is in accord with the existence of antiferromagnetically coupled systems in both cases studied.

Conclusions

The synthesis of three tripodal polyamines is reported. The ligands are based on the well-known structure of the polyamine tris(2-aminoethyl)amine (tren) which has been enlarged with aminopropyl groups (**TAL**) and further functionalized at one of his termini with an anthrylmethyl group (**ATAL**) or at its three termini with naphthylmethyl groups (**N3TAL**). These polyamines interact in aqueous solution with the nucleotide AMP displaying among the highest constants reported in the literature. On the other hand, polyamines **ATAL** and **N3TAL** with aryl groups show higher constants than **TAL**. For **TAL** and **ATAL**, pH-metric titration, ^{31}P NMR measurements and mass spectroscopy evidence the formation of AMP–L species of 2 : 1 and 3 : 1 stoichiometries.

Formation of Cu^{2+} dinuclear complexes are favoured by the presence of the nucleotide which provides additional binding sites for the anchoring of the second metal ion. ^{1}H NMR paramagnetic studies have confirmed the formation of ternary Cu^{2+}–AMP–**TAL** complexes in which AMP behaves as a bridging didentate ligand through its phosphate group.

Experimental

N,*N*′-{2-Bis[2-(3-aminopropylamino)ethyl]aminoethyl}-1,3-propanediamine hexahydrobromide (TAL·6HBr)

N,*N*′-Bis(*p*-tolylsulfonyl-2-aminoethyl)ethane-1,2-diamine (**2**) (6.0 g. 9.9 mmol) and K_2CO_3 (10.9 g, 78.8 mmol) was suspended with 300 mL of CH_3CN. To this mixture was added *N*-(3-bromopropyl)phthalimide (10.9 g. 39.4 mmol) in 150 mL of CH_3CN, then was refluxed for 48 h and filtered off. The solution was vacuum evaporated to dryness and the residue suspended in refluxing ethanol to give **3** as a white solid (yield 89%). Mp: 59–61 °C. ^{1}H NMR ($CDCl_3$): δ_H (ppm) 7.60–7.72 (m, 6H), 7.25 (d, $J = 8$ Hz, 2H), 3.66 (t, $J = 7$ Hz, 2H), 3.16 (t, $J = 7$ Hz, 2H), 3.19 (t, $J = 7$ Hz, 2H), 2.84 (t, $J = 7$ Hz, 2H), 2.37 (s, 3H), 1.90 (dd, $J_1 = 7$ Hz, $J_2 = 7$ Hz, 2H). ^{13}C NMR ($CDCl_3$), δ_C (ppm): 168.0, 143.0, 133.8, 131.9, 129.7, 127.2, 123.5, 123.0, 53.9, 47.0, 46.8, 35.5, 27.4, 21.4.

Compound **3** (5.0 g, 4.26 mmol) was treated with hydrazine hydrate 85% (3 mL) and ethanol (500 mL) and the mixture was refluxed for 24 h, then the resulting solid filtered off. The solution was vacuum evaporated to give (**4**) as an oil (yield 79%). ^{1}H NMR ($CDCl_3$): δ_H (ppm) 7.69 (d, $J = 8$ Hz, 2H), 7.29 (d, $J = 8$ Hz, 2H), 3.11–3.19 (m, 4H), 2.76 (t, $J = 7$ Hz, 2H), 2.72 (t, $J = 7$ Hz, 2H), 2.41 (s, 3H), 1.64–1.71 (m, 2H). ^{13}C NMR ($CDCl_3$), δ_C (ppm): 143.3, 136.2, 129.6, 127.1, 54.4, 47.2, 47.0, 39.0, 32.3, 21.5.

Compound **4** (2.5 g, 3.19 mmol) was suspended with phenol (11.44 g, 121.5 mmol) and HBr–acetic acid 33% (125 mL). The mixture was stirred at 90 °C for 24 h. Then was cooled and the resulting solid was filtered off and washed with ethanol to give *N*,*N*′-{2-bis[2-(3-aminopropylamino)ethyl]aminoethyl}-1,3-propanediamine hexahydrobromide (**TAL**·6HBr) (yield 52%). Mp: 267–271 °C. Anal. Calc. for $C_{15}H_{45}N_7Br_6$: C, 22.44, H, 5.65, N, 12.21. Found: C, 22.5, H, 5.4, N, 12.4%. ^{1}H NMR (D_2O): δ_H (ppm) 3.20–3.31 (m, 4H), 3.12 (t, $J = 8$ Hz, 2H), 2.95 (t, $J = 7$ Hz, 2H), 2.10–2.20 (m, 2H). ^{13}C NMR (D_2O), δ_C (ppm): 49.1, 45.3, 44.9, 36.9, 24.1.

N-9-Anthrylmethyl-*N*′-(2-bis{2-[3-aminopropylamino]ethyl}-aminoethyl)-1,3-propanediamine hexahydrochloride (ATAL·6HCl)

N,*N*′-{2-Bis[2-(3-aminopropylamino)ethyl]aminoethyl}1,3-propanediamine (**TAL**) (1.5 g, 4.8 mmol) and anthracene-9-carbaldehyde (0.8 g, 3.8 mmol) were stirred for 3 h in 75 mL of dry ethanol. $NaBH_4$ (1.8 g, 47.8 mmol) was then added and the resulting solution stirred for 1 h at room temperature. The ethanol was removed under reduced pressure. The resulting residue was treated with water and dichloromethane. The organic phase was removed at reduced pressure and the resulting residue was dissolved in ethanol and precipitated as its hydrochloride salt of *N*-9-anthrylmethyl-*N*-(2-bis{2-[3-aminopropylamino]-ethyl}aminoethyl)-1,3-propanediamine (**ATAL**) (yield 70%). Mp: 217–220 °C

Anal. Calc. for $C_{30}H_{49}N_7$·6HCl: C, 49.60, H, 7.63, N, 13.50. Found: C, 49.4, H, 7.8, N, 13.3%. ^{1}H NMR (D_2O): δ_H (ppm) 8.72 (s, 1H), 8.29 (d, $J = 8$ Hz, 2H), 8.18 (d, $J = 8$ Hz, 2H), 7.74 (dd, $J_1 = J_2 = 8$ Hz, 2H), 7.63 (dd, $J_1 = J_2 = 8$ Hz, 2H), 5.31 (s, 2H), 3.39 (t, $J = 8$ Hz, 2H), 3.15–3.27 (m, 10H), 3.10 (t, $J = 8$ Hz, 6H), 2.92 (t, $J = 6$ Hz, 6H), 2.12–2.22 (m, 6H). ^{13}C NMR (D_2O), δ_C (ppm): 131.1, 129.9, 128.3, 126.0, 123.0, 49.1, 45.2, 45.1, 44.9, 43.6, 36.9, 24.1, 23.0.

emf Measurements

The potentiometric titrations were carried out at 298.1 ± 0.1 K in 0.15 mol dm^{-3} NaCl. The experimental procedure used (burette, potentiometer, cell, stirrer, microcomputer, *etc.*) was the same that has been fully described elsewhere.[19] The acquisition of the emf data was performed with the computer program PASAT.[20] The reference electrode was an Ag/AgCl electrode in saturated KCl solution. The glass electrode was calibrated as an hydrogen-ion concentration probe by titration of previously standardised amounts of HCl with CO_2-free NaOH solutions and determining the equivalent point by the Gran's method,[21] which gives the standard potential, $E^{\circ\prime}$, and the ionic product of water ($pK_w = 13.73(1)$). The concentrations of the different metal ions employed were determined gravimetrically by standard methods.

The computer program HYPERQUAD,[22] was used to calculate the protonation and stability constants. At least three titration curves were performed for each system (*ca.* 100 experimental points). The pH range investigated was 2.5–10.5 and the concentration of AMP and receptors ranged from 3×10^{-4} to a maximun value of 1.5×10^{-3} mol dm^{-3}). The different titration curves for each system were treated either as a single set or as separated curves without significant variations in the values of the stability constants. Several measurements were made both in formation and in dissociation (from acid to alkaline pH and *vice versa*) to check the reversibility of the reactions. The sets of data were merged together and treated simultaneously to give the final stability constants.

In the case of the ternary systems we have performed the following sequence. First, in the data treatment of the ternary systems Cu^{2+}–L–AMP we have included as fixed parameters the protonation constants of AMP,[14] the constants for the formation of Cu^{2+}–AMP complexes[23] and the previously discussed protonation constants of **TAL**, **ATAL** and **N3TAL** (Table 1), those for the system AMP–L (Table 3) and those for the formation of binary Cu^{2+} complexes (Table 2). In this way we have obtained the equilibrium constant shown in Table 4. Secondly, in order to check the consistency of the model, we have then fitted conjointly the titrations of the binary system Cu^{2+}–L and those of the ternary systems Cu^{2+}–L–AMP, leaving as parameters to be refined all the constants for the Cu^{2+}–L and for the Cu^{2+}–L–AMP mixed complexes. The model system obtained was the same in both fittings and the differences between the values of the constants obtained fell within the limits of the standard deviations.

NMR Measurements

The ^{1}H and ^{13}C NMR spectra were recorded on Bruker Avance DPX 300 MHz spectrometer operating at 299.95 MHz for ^{1}H and at 75.43 for ^{13}C. For the ^{13}C NMR spectra, dioxane was used as a reference standard ($\delta = 67.4$ ppm) and for the ^{1}H spectra, the solvent signal. The concentrations of AMP and of the receptors employed in the NMR measurements were in the range 2.5×10^{-4}–10^{-3} mol dm^{-3}. Within the concentration range used, dilution experiments show maximum shifts of the aromatic signals of *ca.*

0.005 ppm discarding significant self-aggregation processes in any of the studied systems.

The ^{31}P NMR spectra were recorded on a Bruker Avance PX 300 MHz operating at 121.495 MHz. Chemical shifts are relative to an external reference of 85% H_3PO_4. Adjustments to the desired pH were made using drops of DCl or NaOD solutions. The pD was calculated from the measured pH values using the correlation, pH = pD − 0.4.[24]

^{1}H paramagnetic NMR measurements were acquired on a Bruker Avance 400 spectrometer operating at 399.91 MHz. One-dimensional spectra were recorded in D_2O solvent with presaturation of the H_2O signal during part of the relaxation delay to eliminate the H_2O signal. Relaxation delay times of 50–200 ms, 30–80 kHz spectral widths ranging and acquisition times of 60–200 ms were used. ^{1}D spectra were processed using exponential line-broadening weighting functions as apodization with values of 20–40 Hz. Chemical shifts were referenced to residual solvent protons of D_2O resonating at 4.76 ppm (298 K) relative to TMS. Sample concentrations for paramagnetic ^{1}H NMR were 2.5 mmol dm^{-3} Cu_2**TAL** complexes. The longitudinal relaxation times of the hyperfine shifted resonances were determined using the inversion recovery pulse sequence $d_1 - 180° - \tau - 90° -$ acq,[25] where d_1 is the relaxation delay and acq the acquisition time), 14 values of τ were selected between 0.4 ms and 300 ms, (d_1 + acq) values were at least five times the longest expected T_1 ranging from 100 to 400 ms, and the number of scans was 8000. The T_1 values were calculated from the inversion–recovery equation. Transversal relaxation times were obtained measuring the line broadening of the isotropically shifted signals at half-height through the equation $T_2^{-1} = \pi\Delta\nu_{1/2}$.

Electrospray mass spectrometry

The electrospray mass spectrum was recorded on a Bruker Esquire 3000plus, Bruker Daltonics mass spectrometer (Agilent Headquarters, Palo Alto, USA). ES-MS was carried out in the positive ion mode. Scanning was performed from m/z = 300 to 1400. For electrospray ionization, the drying gas was set at a flow rate of 2.5 μL min^{-1}, with capillary voltage of 166 V. Non-buffered solutions containing AMP : **TAL** ([**TAL**] = 1.00 × 10^{-3} mol dm^{-3}, molar ratio 6 : 1) in water were injected into the mass spectrometer source with a syringe pump (Cole-Parmer Instruments Company, Illinois, USA) at a flow rate of 2 L min^{-1}. The sampling cone voltage (V_C) was set at 40 V.

Acknowledgements

We would like to thank Prof. H.-J. Schneider for helpful discussion. Financial support from Grupos S03/196 and DGICYT project BQU2003-09215-CO3-01 (Spain) is gratefully acknowledged. J. M. Ll. thanks MCYT of Spain for a Ramón y Cajal contract.

References

1 (*a*) R. M. Izatt, K. Pawlak, J. S. Bradshaw and R. L. Bruening, *Chem. Rev.*, 1991, **91**, 1721; (*b*) A. Bianchi, M. Micheloni and P. Paoletti, *Coord. Chem. Rev.*, 1991, **110**, 17; (*c*) A. Bencini, A. Bianchi, P. Paoletti and P. Paoli, *Coord. Chem. Rev.*, 1992, **120**, 51; (*d*) R. M. Izatt, K. Pawlak, J. S. Bradshaw and L. Bruening, *Chem. Rev.*, 1995, **95**, 2529; (*e*) A. Bianchi, E. García-España and K. Bowman-James, *Supramolecular Chemistry of Anions*, Wiley-VCH, New York, 1997.
2 (*a*) P. A. Gale, *Coord. Chem. Rev.*, 2003, **240**, 191; (*b*) J. M. Llinares, D. Powell and K. Bowman-James, *Coord. Chem. Rev.*, 2003, **240**, 57; (*c*) K. Bowman-James, *Acc. Chem. Res.*, 2005, **38**, 671.
3 A. Metzger, V. A. Lynch and E. V. Anslyn, *Angew. Chem., Int. Ed. Engl.*, 1997, **36**, 862.
4 (*a*) M. Demeunynck, C. Bailly and W. D. Wilson, *Small Molecule DNA and RNA Binders, From Synthesis to Nucleic Acid Complexes*, Wiley-VCH, New York, 2003; (*b*) H.-J. Schneider and A. Yatsimirsky, *Principles and Methods in Supramolecular Chemistry*, Wiley, Chichester, UK, 2000; (*c*) D. Kumar Chand, H.-J. Schneider, J. A. Aguilar, F. Escartí and E. García-España, *Inorg. Chim. Acta*, 2001, **316**, 71; (*d*) H.-J. Schneider and T. Blatter, *Angew. Chem., Int. Ed. Engl.*, 1992, **31**, 1207.
5 For a preliminary report on this behaviour, see: N. Lomadze, E. Gogritchiani, H.-J. Schneider, M. T. Albelda, J. Aguilar, E. García-España and S. V. Luis, *Tetrahedron Lett.*, 2002, **43**, 7801.
6 For a recent review on tripodal amines, see: A. G. Blackman, *Polyhedron*, 2005, **24**, 1.
7 A report on the interaction of the tripodal receptors with nucleic acid models can be seen in: N. Lomadze, H.-J. Schneider, M. T. Albelda, E. García-España and B. Verdejo, *Org. Biomol. Chem.*, 2006, **4**, 1755.
8 M. T. Albelda, E. García-España, L. Gil, J. C. Lima, C. Lodeiro, J. S. De Melo, M. J. Melo, A. J. Parola, F. Pina and C. Soriano, *J. Phys. Chem. B*, 2003, **107**, 6573.
9 (*a*) A. Bencini, A. Bianchi, E. García-España, M. Micheloni and J. A. Ramírez, *Coord. Chem. Rev.*, 1999, **188**, 97; (*b*) C. Frassinetti, L. Alderighi, P. Gans, A. Sabatini, A. Vacca and S. Ghelli, *Anal. Bioanal. Chem.*, 2003, **376**, 1041; (*c*) J. E. Sarnesky, H. L. Surprenant, F. K. Molen and C. N. Reilley, *Anal. Chem.*, 1975, **47**, 2116; (*d*) D. N. Hague and A. D. Moreton, *J. Chem. Soc., Perkin Trans. 2*, 1994, 265.
10 R. M. Smith and A. E. Martell, *NIST Stability Constants Database, version 4.0 National Institute of Standards and Technology*, Washington, DC, 1997.
11 (*a*) F. Thaler, C. D. Hubbard, F. W. Heinemman, R. Van Eldik, S. Schlinder, I. Fábian, A. M. Dittler-Klingemann, F. E. Hahn and C. Orvig, *Inorg. Chem.*, 1998, **37**, 4022; (*b*) J. R. Hartam, R. W. Bachet, W. Pearson, R. J. Wheat and J. H. Callahan, *Inorg. Chim. Acta*, 2003, **343**, 119.
12 G. Anderregg and V. Gramlich, *Helv. Chim. Acta*, 1994, **77**, 685.
13 The logarithms of the protonation constants in 0.15 mol dm^{-3} $NaClO_4$ at 298.1 K are: $\log K_{HL/H\cdot L} = 10.39(3)$, $\log K_{H_2L/HL\cdot H} = 10.33(3)$, $\log K_{H_3L/H_2L\cdot H} = 9.64(2)$, $\log K_{H_4L/H_3L\cdot H} = 8.89(2)$, $\log K_{H_5L/H_4L\cdot H} = 8.02(2)$, $\log K_{H_6L/H_5L\cdot H} = 7.39(2)$.
14 Protonation constants for AMP determined at 298.1 K in 0.15 mol dm^{-3} NaCl: $\log K_{HL/H\cdot L} = 6.32(1)$; $\log K_{H_2L/HL\cdot H} = 10.26(1)$.
15 For a recent review on anion coordination chemistry, see for instance: S. Kubik, C. Reyheller and S. Stüwe, *J. Inclusion Phenom. Macrocycl. Chem.*, 2005, **52**, 137.
16 C. Miranda, F. Escartí, L. Lamarque, E. García-España, P. Navarro, J. Latorre, F. Lloret, H. R. Jiménez and J. R. Yunta, *Eur. J. Inorg. Chem.*, 2005, 189.
17 B. Verdejo, J. Aguilar, A. Doménech, C. Miranda, P. Navarro, H. R. Jiménez, C. Soriano and E. García-España, *Chem. Commun.*, 2005, 3086.
18 M. Bera, W. T. Wong, G. Aromi and D. Ray, *Eur. J. Inorg. Chem.*, 2005, 2526.
19 E. García-España, M.-J. Ballester, F. Lloret, J.-M. Moratal, J. Faus and A. Bianchi, *J. Chem. Soc., Dalton Trans.*, 1988, 101.
20 M. Fontanelli and M. Micheloni, *Proceedings of the Spanish-Italian Congress on Thermodynamic of Metal Complexes*, Diputación de Castellón, Castellón, Spain, 1990.
21 G. Gran, *Analyst*, 1952, **77**, 661; F. J. C. Rossotti and H. Rossotti, *J. Chem. Educ.*, 1965, **42**, 375.
22 P. Gans, A. Sabatini and A. Vacca, *Talanta*, 1996, **43**, 1739.
23 E. Martell, R. M. Smith and R. J. Motekaitis, *NIST Critically Selected Stability Constants of Metal Complexes Database, NIST Standard Reference Database, version 4*, 1997.
24 A. K. Convington, M. Paabo, R. A. Robinson and R. G. Bates, *Anal. Chem.*, 1968, **40**, 700.
25 R. L. Vold, J. S. Waugh, M. P. Klein and D. E. Phelps, *J. Chem. Phys.*, 1968, **48**, 3831.